

Effect of fluorine doped TiO₂ on the property of perovskite solar cell

X Q Zhang¹, Y P Wu¹, Y Huang^{1,2}, Z H Zhou^{1,2,*} and S Shen³

¹ College of Materials, Xiamen University, Xiamen, Fujian, China 361005

² Fujian Key Laboratory of Advanced Materials, Xiamen, Fujian, China 361005

³ CSIRO Manufacturing, Clayton, VIC 3168, Australia

E-mail: *zzh@xmu.edu.cn

Abstract. Anatase TiO₂ nanoparticles with different amounts of fluorine doping were synthesized by a hydrothermal method using hydrogen titanate nanotubes as a precursor and applied as mesoporous layer for preparing perovskite solar cell. The morphology and structures were characterized by scanning electron microscope (SEM) and X-ray diffraction (XRD), meanwhile, the properties and performances were tested by photoluminescence spectrum (PL) and current density and voltage (J-V) curve. It was found that doping fluorine into TiO₂ made the photoelectric conversion efficiency (PCE) of perovskite solar cell (PSC) to be improved. The best PCE of PSC based on a F-doped TiO₂ was 13.06% and increased by 51% compared to an un-doped TiO₂. The study provided a direction for the exploration of high performance electron transport layer of perovskite solar cell.

Keywords: perovskite solar cell, TiO₂ mesoporous layer, fluorine doping

1. Introduction

Perovskite solar cell (PSC) is one of the most promising next-generation solar cells. Due to the energy band structure matching between TiO₂ and perovskite, photoelectrons can be effectively extracted and transported by the TiO₂ mesoporous layer into PSC. Therefore, modification of TiO₂ mesoporous material is an important approach to control the conversion efficiency of PSC [1-4].

It is well known that element doping is an effective way for TiO₂ modification. Yoshida etc. [5] fabricated Mg-doped anatase TiO₂ nanorods with a microwave hydrothermal method and applied them as the PSC mesoporous layer. They explained that magnesium doping widened the TiO₂ band gap, and improved the degree of the energy band structure matching between TiO₂ and perovskite, which promoted the electron transfer ability of TiO₂, and increased the PSC conversion efficiency by 33%. Other metal element doping, such as Nb-TiO₂ [6], Y-TiO₂ [7], Sn-TiO₂ [8] etc., have also been successively reported. However, the above literatures rarely mentioned the issue of oxygen vacancy, which leads to the existence of "trap state" between the band gaps of TiO₂. It is known that the "trap state" caused by oxygen vacancy in TiO₂ is considered as the disadvantage of charge transfer because of the photoelectron capture for the TiO₂ mesoporous layer in PSC [9-11]. Hence, studying the issue of oxygen vacancy is significant work for the development of PSC.

We have reported the preparation of F-doped TiO₂ and its application for PSC, and found that the oxygen vacancy in TiO₂ could be greatly reduced by the fluorine doping process [12]. It is deduced that one O²⁻ ion needs to be replaced by two F⁻ ions, and one F⁻ ion takes O²⁻ position but another F⁻ ion may be possible to fill into the oxygen vacancy existing in the TiO₂ lattice. As a result, the oxygen



vacancy is reduced and the electron transport performance of the TiO₂ is improved. It is the reason that the property of PSC is boosted [12]. For further optimization of F-doping, in this study, we explored TiO₂ with different fluorine doping amounts for the mesoporous layer of PSC and discussed the effect of fluorine doping amounts on the photoelectron conversion efficiency (PCE) of PSC.

2. Experimental

2.1. Materials preparation

All the chemical reagents used are of analytical grade without further purification. The preparation method of F-doped TiO₂ is a modified version reported previously [12], in a typical run: 1 g of P25 TiO₂ powders was dispersed in 75 ml of 10 M NaOH solution, the mixture was injected into a 100 ml autoclave and heated to 130°C for 24 h. After cooled down to room temperature, the as-obtained precipitation was washed and centrifuged with dilute nitric acid and distilled water for several times, then dried at 80°C overnight, and hydrogen titanate precursor powders were obtained. Afterwards, 1 g hydrogen titanate precursor mixed with 0, 0.25, 0.5 and 1 g KBF₄, respectively, were added into 75 ml 0.01 M nitric acid solution. The resulted solution was transferred to a 100 ml autoclave and heated to 180°C for 24 h, then washed and centrifuged with distilled water and ethanol for several times and dried overnight. The different F-doped TiO₂ samples were obtained and remarked as S0, S1, S2, S3 and S4, accordingly. Finally, all F-doped TiO₂ slurries were prepared according to the method reported in other work [13].

2.2. Perovskite solar cell fabrication

F-doped SnO₂(FTO) substrates were ultra-sonicated and washed in turn by acetone, isopropyl alcohol and distilled water respectively for 10 minutes. TiO₂ density layer with a thickness of about 60 nm was deposited by spin coating with a rate of 4000 r/s for 30 s using the titanium diisopropoxide bis(acetylacetonate) solution and calcinated at 500°C for 30 min. TiO₂ mesoporous layer with a thickness of about 200 nm was deposited by spin coating with a rate of 4000 r/s for 30 s using the as-prepared TiO₂ slurry and calcinated at 500°C for 30 min. Then, perovskite layer was coated by a standard two-step spin coating process. Firstly, a 460 mg ml⁻¹ PbI₂ DMF solution was coated on the mesoporous TiO₂ layer with a speed of 3000 r/s for 30 s. Secondly, 20 mg ml⁻¹ MAI solution was coated with the same spin speed and time. The substrate was dried with a plate at 100°C for 10 min, the HTM (Spiro-MeOTAD) layer was coated with a speed of 3000 r/s for 30 s. Finally, Ag electrode with a thickness of 100 nm was evaporated thermally on the top of the device.

2.3. Testing and characterizations

Bruker AXS (D8 advance) X-ray diffraction was used to analyze the phase structure of the samples, the spectra were collected under the following conditions: Irradiated with graphite monochromatic copper λ (Cu, K α) = 0.154 nm, at 40 kV and 40 mA over a range of 10~90° with a step of 0.0167° for 0.1 s. Scanning electron microscope (SEM, Hitachi SU-70, 10 kV) was used for morphology characterization. Current density and voltage curve (J-V) were measured under a solar intensity of AM 1.5, including a 450 W xenon lamp light source (Newport 6279 ns) and a Keithley 2400 source table. The photoluminescence characterization was conducted by using fluorophotometer (Fluoromax-4c, HORIBA) in the range of 700-830 nm with an excited wavelength of 460 nm.

3. Results and discussion

Figure 1(a) shows the XRD patterns of the different TiO₂ samples. The peaks of all patterns are in accord with the lattice planes of anatase TiO₂ listed in the PDF#73-1764 card, confirming the formation of anatase TiO₂ in all cases. Besides, some peaks, in accord with KBF₄, appear in the S4 pattern. The average grain sizes are obtained by the Scherrer equation [14] and the values of all TiO₂ samples are listed in the Table 1. It demonstrates that the grain size of TiO₂ changes slightly by the fluorine doping.

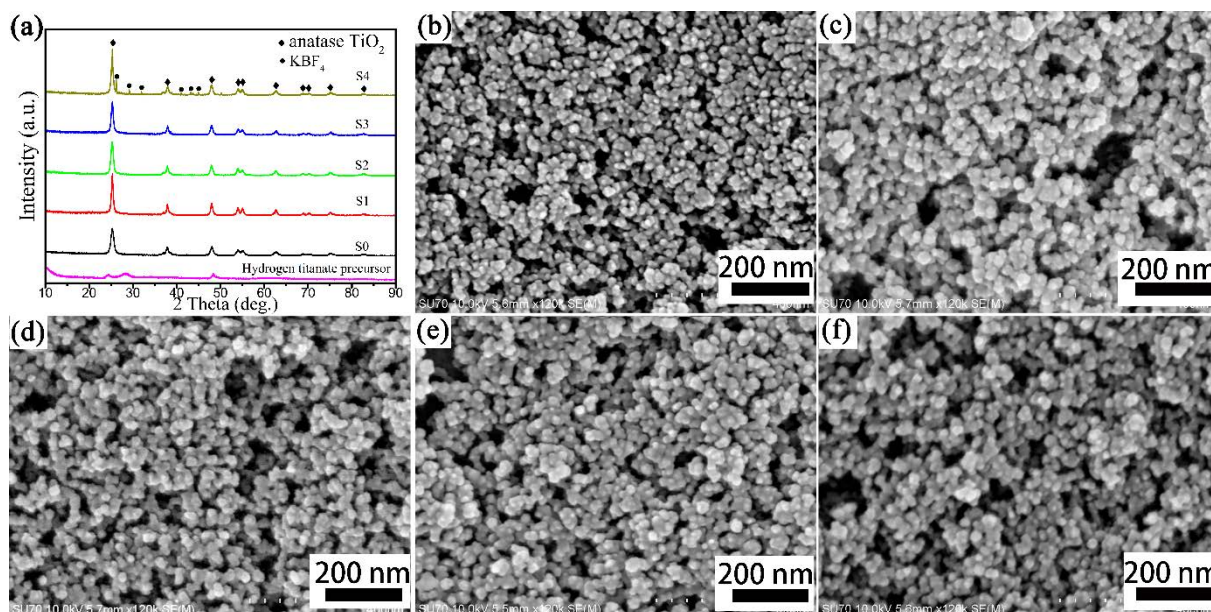


Figure 1. XRD patterns (a) and SEM images of the different TiO₂ samples (b:S0, c:S1, d:S2, e:S3, f:S4).

The SEM images of the different TiO₂ samples were shown in figure 1(b) ~ (f). It is obvious that all samples possess the similar uniform grain size of about 10 ~ 20 nm, and the results agree to the above XRD results. According to XRD and SEM results, it is confirmed that the fluorine doping in TiO₂ does not affect the grain size of the TiO₂ particles.

How does the fluorine doping in TiO₂ affect the property of perovskite solar cell? The PSC with the different TiO₂ samples as mesoporous layer were prepared with the same process [15], the J-V curves (shown in figure 2(a)) of all PSC were tested under AM1.5 light intensities similarly, and the relative parameters are also shown in table 1. It is obvious that the PCE of the PSC based on S0 is 8.63%, by contrast, the PCE of the PSC based on S1 ~ S3 improve dramatically. The PCE of the PSC based on S3 reaches a maximum of 13.06%, which boosted by 51.3% compare to S0. Meanwhile, the PCE of the PSC based on S4 declines distinctly, which can be explained by the above XRD result. XRD peaks of KBF₄ have been confirmed in the XRD pattern of S4 (figure 1(a)). So there exists some surplus KBF₄ in sample S4. The surplus KBF₄ may be adsorbed on the surface of the TiO₂ grain, which will hinder the photoelectron transport between TiO₂ grains, resulting the notably decline of PCE of PSC.

Table 1. Grain size of the different TiO₂ samples and the property of PSC.

Samples	crystal size (nm)	J _{sc} (mA/cm ²)	V _{oc} (V)	FF	PCE (%)
S0	9.9	20.97	0.98	0.42	8.63
S1	11.2	21.67	0.98	0.43	9.13
S2	10.9	22.97	1.01	0.52	12.06
S3	10.4	24.40	1.01	0.53	13.06
S4	11.0	18.63	0.98	0.35	6.39

For further confirming that the fluorine doping improves the electron transport of TiO₂ and leads the boost of the PCE, the photoluminescence (PL) spectrum test of different TiO₂/perovskite (PVSK) were carried out and the results are shown in figure 2(b). It is observed that all PL spectra show an evident peak near 760 nm, which is accord with other reports [16-18]. The order of the peak intensity is PVSK > (S4/PVSK) > (S0/PVSK) > (S1/PVSK) > (S2/PVSK) > (S3/PVSK), demonstrating that the order of efficiency of photo-generated electron extraction and transport is S3 > S2 > S1 > S0 > S4, which agrees with above J-V result.

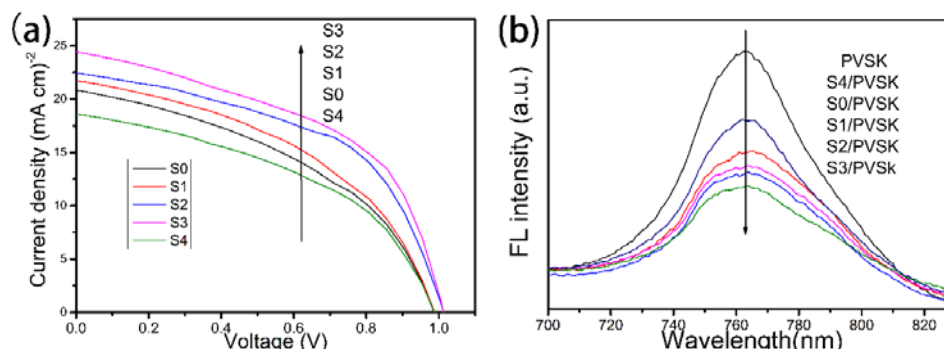


Figure 2. (a) the J-V curve of the PSC with different TiO₂ samples and (b) the photoluminescence spectrum of different TiO₂/PVSK devices.

4. Conclusion

F-doped TiO₂ samples with different fluorine doping amounts were prepared by a two-step hydrothermal method. Compared to the un-doped TiO₂, F-doped TiO₂ can not only maintain the TiO₂ crystal type and grain size, but also improve the electron transport ability of TiO₂. When F-doped TiO₂ samples were applied as the mesoporous layer of PSC, the PSC with sample S3 possesses a maximum PCE of 13.06%, which boosts by 51.6% comparing to that with un-doped TiO₂. It demonstrates that doping fluorine into TiO₂ is an effective means to improve the PCE of PSC. The above study may provide a direction for the exploration of high performance electron transport layer of PSC.

Acknowledgment

This work is supported by the Science and Technology Major Program (2014HZ0005) of Fujian Province, China.

References

- [1] Kojima A, Teshima K, Shirai Y and Miyasaka T 2009 *J. Am. Chem. Soc.* **131** 6050
- [2] Grätzel M 2014 *Nat. Mater.* **13** 838
- [3] Sum T C and Mathews N 2014 *Energy Environ. Sci.* **7** 2518
- [4] Saliba M *et al.* 2016 *Energy Environ. Sci.* **9** 1989
- [5] Manseki K, Ikeya T, Tamura A, Ban T, Sugiura T and Yoshida T 2014 *RSC Adv.* **4** 9652
- [6] Yang M, Guo R, Kakel K, Liu Y, O'Shea K, Bone R, Wang X, He J and Li W 2014 *J. Mater. Chem. A* **2** 19616
- [7] Qin P *et al.* 2014 *Nanoscale* **6** 1508
- [8] Zhang X, Bao Z, Tao X, Sun H, Chen W and Zhou X 2014 *RSC Adv.* **4** 64001
- [9] Konr F J, Mercado C C and McHale J J 2008 *J. Phys. Chem. C* **112** 12786
- [10] Gopal N O, Lo H-H, Ke T-F, Lee C-H, Chou C-C, Wu J-D, Sheu S-C, and Ke S-C 2012 *J. Phys. Chem. C* **116** 16191
- [11] Hurum D C, Agrios A G, Crist S E, Gray K A, Rajh T and Thurnauer M C 2006 *J. Electron. Spectrosc. Relat. Phenom.* **150** 155
- [12] Zhang X, Wu Y, Huang Y, Zhou Z and Shen S 2016 *J. Alloys Compd.* **681** 191
- [13] Lee J, Lee T, Yoo P J, Grätzel M, Mhaisalkar S and Park N 2014 *J. Mater. Chem. A* **2** 9251
- [14] Tripathi A K, Mathpal M C, Kumar P, Singh M K, Soler M A G and Agarwal A 2015 *J. Alloys Compd.* **622** 37
- [15] Burschka J, Pellet N, Moon S, Baker R H, Gao P, Nazeeruddin M K and Grätzel M 2013 *Nature* **499** 316
- [16] Liu D, Yang J and Kelly T L 2014 *J. Am. Chem. Soc.* **136** 17166
- [17] Xie Y, Shao F, Wang Y, Xu T, Wang D and Huang F 2015 *ACS Appl. Mater. Interfaces* **7** 12937
- [18] Sun S, Salim T, Mathews N, Duchamp M, Boothroyd C, Xing G, Sum T C and Lam Y M 2014 *Energy Environ. Sci.* **7** 399